Electronically Reconfigurable Transmitarray at Ku Band for Microwave Applications

Pablo Padilla, Alfonso Muñoz-Acevedo, Manuel Sierra-Castañer, *Member, IEEE*, and
Manuel Sierra-Pérez, *Senior Member, IEEE*

Abstract—An electronically reconfigurable transmitarray device at 12 GHz is presented in this work. This paper highlights the functioning of this kind of device and thoroughly examines the proposed reconfigurable transmitarray. The architecture is discussed along with the design and selection of all the constituting elements and the prototypes for all of them. In order to add reconfigurability to the transmitarray structure, 360° reflective phase shifters were designed, prototyped and validated for direct application. Eventually, a demonstrative prototype for an active transmitarray with phase shifters was assembled, and radiation pattern measurements were taken in an anechoic chamber to demonstrate the capabilities of this structure.

Index Terms—Antenna array, constrained lens, directional coupler, Ku band, microstrip circuit, microstrip technology, patch antenna, phase shifter, phase shifting, reflective circuitry (RTPS), transmitarray, varactor.

Fig. 1. Scheme of transmitarray general functioning.

I. INTRODUCTION

IN the technical world, in the area of antennas and radiating systems, there is growing interest in lens-type or reflector-type structures called transmitarrays and reflectarrays, respectively. These structures replace and, in certain cases, improve the outcomes of traditional structures, such as reflectors or lenses, depending on the considered structure.

The focus of this paper is in active transmitarray structures, also called artificial or constrained lenses [1]. In particular, a transmitarray architecture is proposed and defined. All the constituting elements of the proposed transmitarray lens architecture are designed, prototyped and measured, and, for the sake of completeness, the design and manufacture of one transmitarray demonstrator is offered.

The paper is organized as follows. This section (Section I) describes the scope of this work and its relationship to previously published papers. Section II offers the complete active transmitarray characterization and design, and introduces the forming elements, divided into passive and active. Section III attends to these passive transmitarray forming devices, and Section IV at-
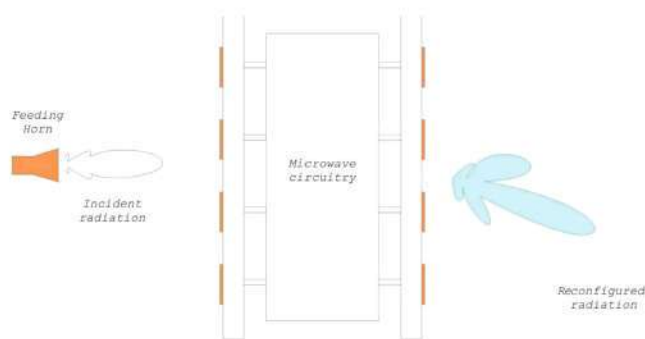
tends to active ones (phase shifters). Section V describes the assembly and measurements of the first active transmitarray manufactured prototype, considered as a first demonstrator of this kind of artificial lens device. The clear purpose of this first prototype, and the main contribution of this work, is to demonstrate the feasibility of the proposed active device and its architecture for proper functionality, according to its expected theoretical behavior. The design of the active devices presented in this work (Section V) is another main contribution of this document. Finally, in Section VII, conclusions are drawn.

The basics of transmitarray lens structures are easily understood: first, an electromagnetic wave (with specific wave-front properties) is received by the reception interface of the lens, and then the received signal is processed in a particular way (phase shift, amplification, etc.). Eventually, the processed signal is retransmitted with new wave-front properties due to the modifications introduced in the processing stage, as sketched in Fig. 1.

Various transmitarray approaches have been described in the literature. Fundamental principles regarding active lenses are offered in [2] and [3]; active lenses for radar applications (HAPDAR project) have been heavily studied. Quite relevant are the models proposed in [1] and [4]. Some of these models are used in a multi-beam working scheme [4]: the main beam direction differs depending on the position of the feeder related to the lens. Regarding circuitry used to deal with received signals, lenses are classified into active lenses (if an external control signal is used for the inner circuitry configuration) [2]–[4] or passive lenses (with no circuitry reconfiguration) [6]–[8]. This paper focuses on the design and manufacture of a complete active microwave lens and also describes an electronically reconfigurable lens demonstrator.

One of the main values in this kind of devices, despite the multi-beam functionality, consists of placing it in front of a particular antenna, which offers two key advantages.
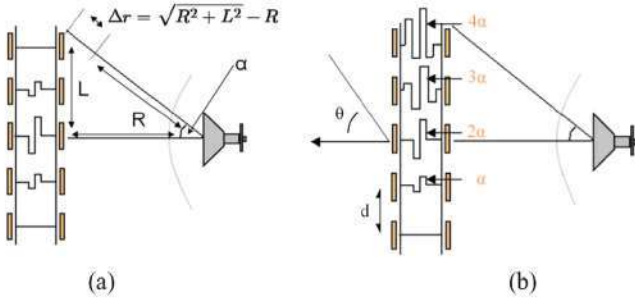
Fig. 2. The transmitarray main advantages. (a) Phase error correction. (b) Radiation pattern reconfiguration.

- Phase error correction due to the spherical wave front coming from the feeding antenna;
- New radiation pattern configuration, modifying the phase response of each forming transmitarray cell.

Fig. 2 highlights these two effects.

Transmitarray lens feeders are important in the design of the final lens. Feeders with different radiation properties are used in this kind of constrained lenses, affecting the resulting radiation pattern of the lens. Some effects (such as taper) are difficult to introduce in conventional phased arrays without a high level of complexity (consider, for instance, the complexity in the introduction of a particular taper that is given by the feeder in the case of a transmitarray lens).

II. COMPLETE ACTIVE TRANSMITARRAY CHARACTERIZATION AND DESIGN

The transmitarray structure is divided into two principal parts: the radiating interface for reception and transmission and the processing interface for array phase conformation in each transmitarray cell. This active transmitarray demonstrator has been designed to work with linear polarization at 12 GHz and a bandwidth of 0.7 GHz. The phase shifters have been designed with a range of phase variation greater than 360° in order to enable possible electronic tilt in the H and V planes independently. For this demonstrative prototype, an existing conical corrugated horn has been used as a feeder; this implies that the spillover efficiency of the design has not been optimized. Moreover, in this prototype, due to the simplicity of the fabrication process, the radiating elements are grouped into sets of four elements, so the scan capability is limited.

With a transmitarray structure with planar technology, the greatest challenge is the placement of the processing interface inside the structure, between both radiating interfaces, because of the limited space available. Both of the interfaces (processing and radiating) that form the transmitarray are designed in planar architecture over the ground plane. If the interconnection point is freed from this restriction (planar connection), making it possible to change the reference plane for each interface by means of perpendicular connection, the space constraint in one of the dimensions is considerably reduced. Thus, microstrip lines for the processing interface can be applied. However, the requirements for the other dimensional components are strictly the same. Fig. 3 illustrates this fact, with the perpendicular connection between planar interfaces.
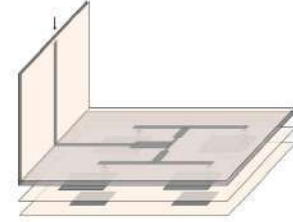

Fig. 3. Scheme of the interconnection between the processing interface and the radiating one, with 90° change in reference plane.
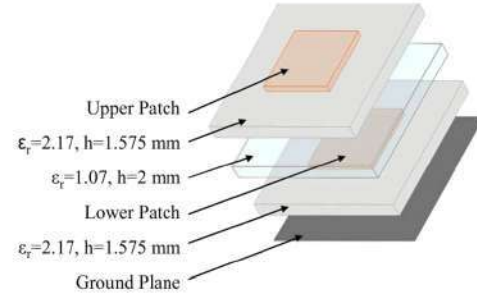

Fig. 4. Model for patch design, in layer scheme.

In the defined architecture for the complete structure, the complexity of connecting the stacked patch array structures for transmission and for reception by means of microstrip lines is condensed in the interconnection point. Fig. 3 reveals the necessity of designing a transition between coaxial-type patch connections and microstrip transmission lines, along with the necessity of designing a 90° transition with reference plane change in the microstrip line.

Thus, the structure is divided into passive elements (radiating elements, one to four distribution networks and 90° transitions), and active elements (phase shifters).

III. PASSIVE TRANSMITARRAY ELEMENT DESIGN, SIMULATION AND PROTOTYPING

A. Radiating Element

For the radiating elements, patches were selected for their planar structure, a geometry that is especially suitable for transmitarray devices. In order to improve certain features, multilayer stacked patch elements over the ground plane were used rather than simple patch ones because of their wider working frequency band. CST Microwave Studio 2006 was used for the design stage. Fig. 4 depicts the layer distribution and materials employed.

In the design process, one isolated stacked patch and one stacked patch embedded in an array are separately considered, the latter including mutual coupling effects with surrounding patches. Fig. 5 shows this prototype, the design and measured results.

B. Distribution Network

A one-to-four bidirectional distribution network in a microstrip line was designed, sharing the ground plane with the radiating structure (and below it). Prototypes for the distribution network exhibited adequate behavior, as seen in Fig. 6.
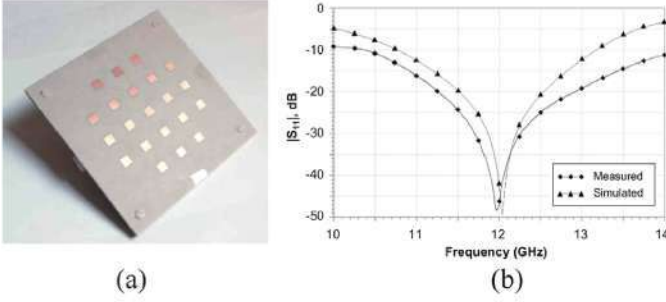
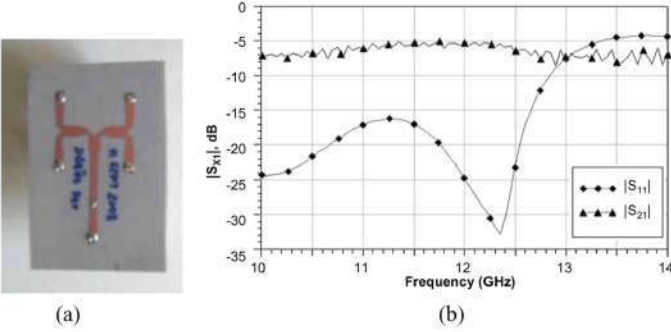Fig. 5. Stacked patch embedded in array. (a) Prototype. (b) Simulated and measured results.

Fig. 6. Prototype of distribution network. (a) Prototype. (b) $|S_{11}|$ and $|S_{21}|$.
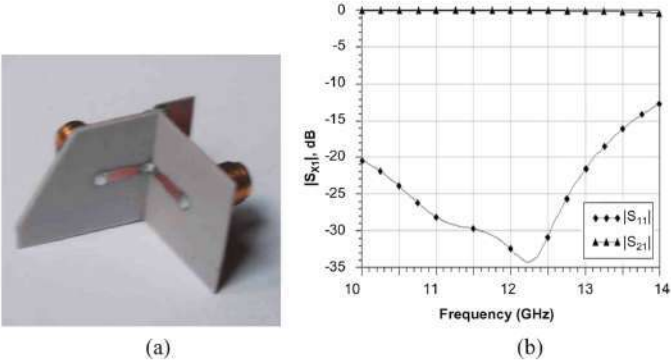

Fig. 7. Reference plane change. (a) Prototype. (b) $|S_{11}|$ and $|S_{21}|$.

C. Reference Plane Change

The transition with reference plane change was characterized and designed. Fig. 7 shows the prototype results for this transition.

IV. ACTIVE ELEMENT: 360° ELECTRONICALLY TUNABLE PHASE SHIFTER DESIGN AND PROTOTYPING

One way to design a 360° phase shifter is to design a device with varactors as tunable elements [9]. In order to introduce phase variation by capacitance changes, two devices are placed together: a four-port directional coupler and reflective circuits (LC circuit). The resulting circuit, a combination of these two circuits, is a two-port device that combines the signal in a particular way to obtain an output signal that is the same as the input signal with a phase variation. In conventional use, all the devices connected to the directional coupler have to be properly matched
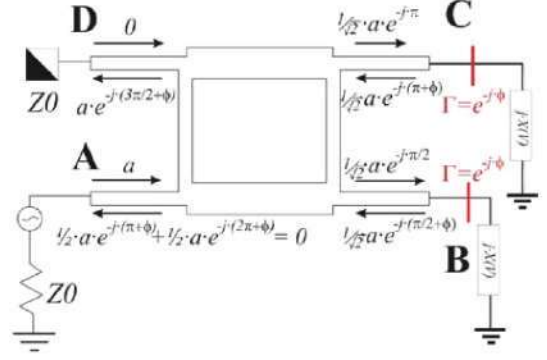

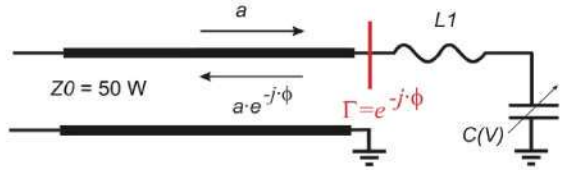Fig. 8. Phase shifter complete model, with tunable circuits at ports B and C.

Fig. 9. Detail of the tunable circuit at ports B and C.

to obtain the common directional coupler behavior. However, considering port A (see Fig. 8) as the input port, if open circuits are placed in ports B and C, all the signals arising in ports B and C are reflected, re-entering the directional coupler, with ports A and D as new output ports. The configuration of the directional coupler forces in ports D and A obtain the sum in phase and the sum in opposite phase, respectively, of the reflected signals coming from ports B and C.

If the open circuits in ports B and C are changed, and tunable LC circuits are placed, the phase of the reflected signal in ports B or C can be varied. As a consequence, all the input power from port A is redirected to port D and the resulting signal in port D differs in phase from the original one in port A, owing to the correction introduced by the tunable circuit, as shown in Fig. 8. It is essential to guarantee symmetry in the complete device: the same circuit (with the same phase behavior) must be placed in ports B and C in order to force the sum in phase and in opposite phase in ports D and A, respectively.

As main features of the device, the phase variation range must be greater than 360 degrees, while the losses must be minimized (i.e., better than −3 dB).

A. Reflective Circuit Design and Simulation

The circuit connected in ports B and C behaves (for the working frequency range) as a completely mismatched circuit, reflecting the entire received signal. It is necessary to have an equivalent impedance with no real part in order to obtain the maximum value for the reflection coefficient, as shown in (1). Thus, an adequate tunable LC circuit (with a varactor controlled in voltage (V) as capacitance) could satisfy these constraints, as shown in Fig. 9

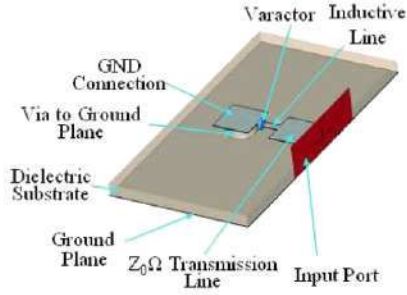$$|\Gamma| = \frac{|jX(V) - Z_0|}{|jX(V) + Z_0|}. \tag{1}$$

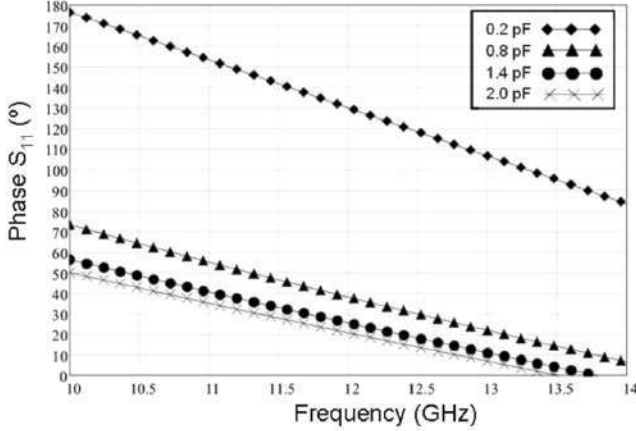Fig. 10. Simulation model for the equivalent printed LC circuit.

Fig. 11. Simulated phase variation for the reflective circuit.

Fig. 12. Complete simulation model for the phase shifter.

Fig. 13. Simulated $|S_{11}|$ parameter for the complete phase shifter.

One of the most important constraints in the design of the device is the usage of lumped elements (inductors, capacitors) at Ku band (12 GHz in this case) with low parasitic effects. Capacitors are replaced by varactors for microwave purposes while inductances are designed using equivalent high-impedance microstrip printed circuits, working as inductances in the working frequency range [10], [11]. In this case, the varactors are the only lumped elements in the complete device.

To obtain the behavior of an LC circuit, printed technology for the inductors was applied and varactors for the capacitors were used. Fig. 10 shows the simulation model in detail, with ground plane connections, printed inductive lines and varactors as the unique lumped elements.

Once the model is properly designed, the simulations yield the results shown in Fig. 11 for the expected phase response for different capacitance values (taking linear capacitance variation within the valid range of the varactor selected).

The range of capacitances available in the varactor yields a reflective circuit with ~140-degree variation in the best case. As discussed later, in the complete phase shifter simulation, it is mandatory to replicate the reflector and coupler set (denoted 'primary cell' from now on) up to three times to reach the 360-degree variation.

B. Complete Phase Shifter Design and Simulation

The phase shifter was designed using directional couplers. These have been designed as conventional −3 dB/90 deg couplers with no extra features, in microstrip technology (as for the rest of the device). Some design techniques are found in [12]–[14].
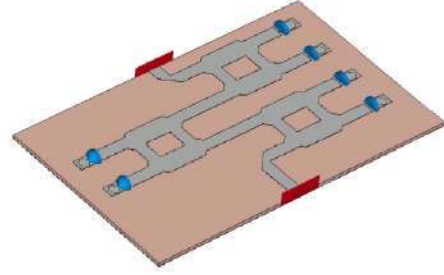
As mentioned before, the designed and simulated coupler with reflective circuits set achieves an insufficient phase variation, according to the main specifications. This constraint could be overcome with the replication of the primary cell, as exemplified in Fig. 12.

The final device has two ports (input and output), with no outer access to the ports with reflective circuits. For the sake of simplicity, the capacitance values for all the varactors are the same. In this case, the control voltage for each varactor is the same (only one control voltage for the entire phase shifter). Figs. 13 and 14 exhibit reflection ($|S_{11}|$) at the input port and transmission ($|S_{21}|$) from the input port to the output port, respectively, in terms of S-parameters, for different capacitance values.

Fig. 15 shows the phase variation ($\arg(S_{21})$) achieved with the final designed phase shifter.

The phase variation versus the capacitance value for the varactors is shown in Table I.

C. Phase Shifter Prototype and Measurement

As mentioned, the most important element of the device is the reflective circuit. The varactor selected for the variable capacitor in the reflective circuit is the M/A-COMMA46585–1209. The varactor mounting constraints for avoiding damage force a low soldering temperature: either bounding techniques or conductive epoxy soldering techniques satisfy these constraints. The latter technique is chosen. Some details are shown in Figs. 16 and 17.

Transmission and reflection parameters are obtained; S parameters in terms of amplitude are shown in Fig. 18. Phase behavior is shown in Fig. 19.

Capacitance Value	Voltage	Simulated phase (°)	Measured phase (°)
2 pF	0 v	0	0
1.5 pF	1 v	-12	-11
0.95 pF	2 v	-31	-29
0.65 pF	3 v	-55	-55
0.5 pF	4 v	-81	-82
0.4 pF	5 v	-110	-114
0.34 pF	6 v	-139	-144
0.29 pF	7 v	-168	-173
0.26 pF	8 v	-197	-200
0.23 pF	9 v	-224	-227
0.21 pF	10 v	-254	-256
0.20 pF	11 v	-280	-283
0.19 pF	12 v	-304	-310
0.17 pF	13 v	-326	-336
0.167 pF	14 v	-345	-354
0.159 pF	15 v	-362	-372
0.152 pF	16 v	-378	-392

Fig. 14. Simulated $|S_{21}|$ parameter for the complete phase shifter.
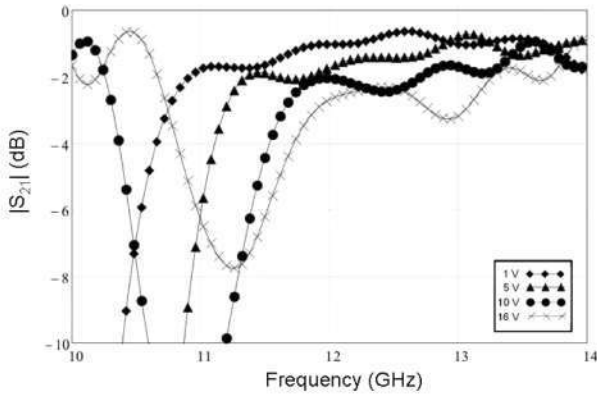

Fig. 16. Complete prototype for the phase shifter.

Fig. 15. Simulated phase variation for the complete phase shifter. Edge values.
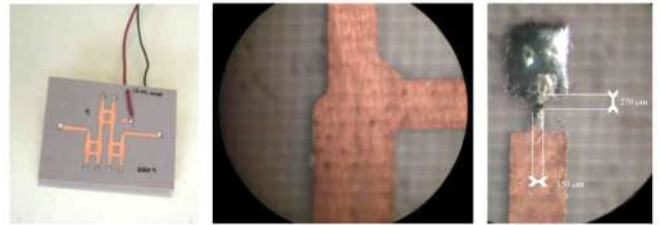
Fig. 17. Details of the prototype for the phase shifter.

A quite linear phase/voltage relation is obtained, as shown in Table I.

V. COMPLETE ACTIVE TRANSMITARRAY SCAN CAPABILITY SIMULATED RESULTS

As mentioned previously, the radiation elements have been combined in groups of four in order to simplify the construction of this prototype. With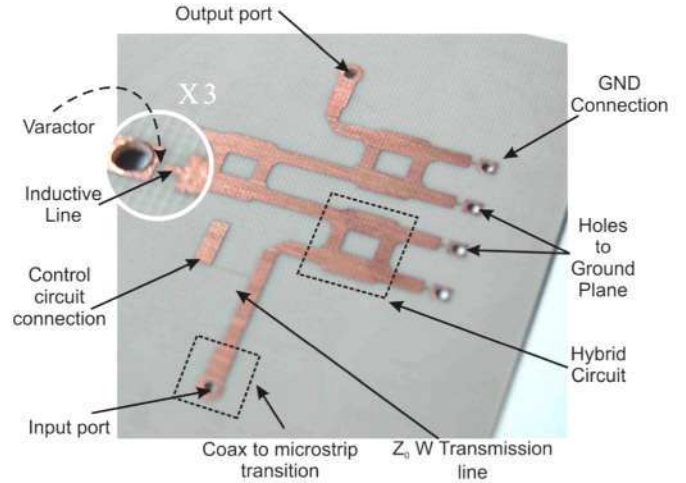 this configuration, the separation between groups of four patches is equal to 1.4 wavelengths. The consequence of this constraint is the reduction in the scan capability of the whole array due to the grating lobes of the structure. However, if a scan range greater than 10 deg. is required, one phase shifter per radiation element should be used. Fig. 20 shows the simulated radiation pattern for steering angles of 0, 10 and 15 deg. The −3 dB beam width remains almost constant and equal to 12.1 deg in all these cases. In the last case, the grating lobes completely disrupt the pattern. For that reason, the
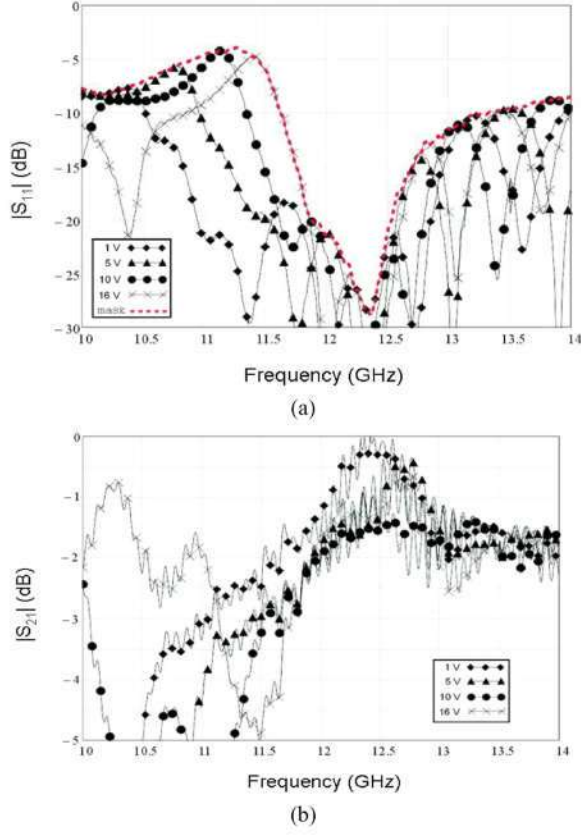
(a)

(b)

Fig. 18. Phase shifter measurements. (a) Measured $|S_{11}|$ variation for the prototype for different control voltages. (b) Measured $|S_{21}|$ variation for the prototype for different control voltages.
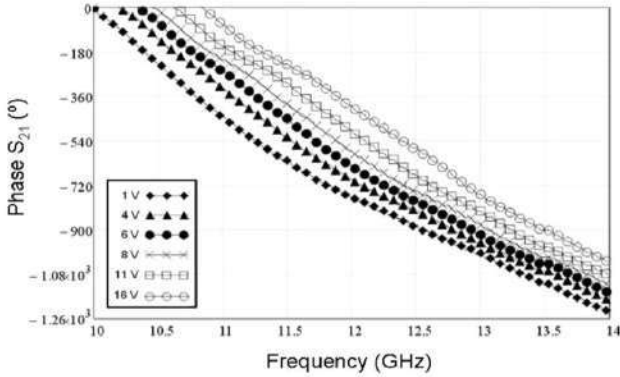

Fig. 19. Measured phase variation for different control voltages.

prototype has been characterized, for demonstrative purposes, at steering angles of 0 deg and 9 deg.

VI. COMPLETE ACTIVE TRANSMITARRAY ASSEMBLY AND MEASUREMENT RESULTS

Globally, the assembly for each active transmitarray cell includes the four-to-one distribution network, the transition device between the coaxial-type feeding at each patch and the microstrip structure of the distribution network, as diagrammed in Fig. 21.
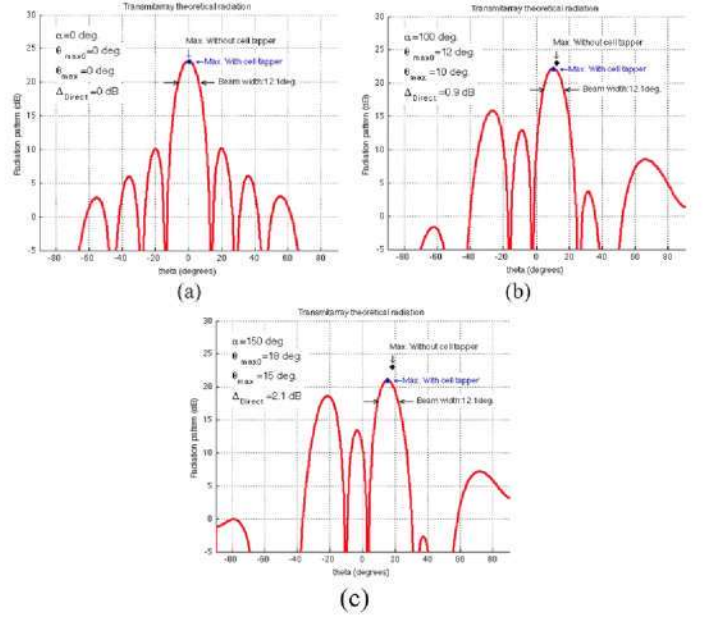

(a)   (b)

(c)

Fig. 20. Simulated radiation pattern for different steering angles. (a) 0 deg. (b) 10 deg. (c) 15 deg.
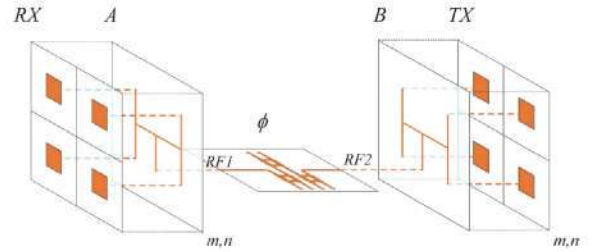

Fig. 21. Assembly model for a four-patch transmitarray cell.

(a)   (b)
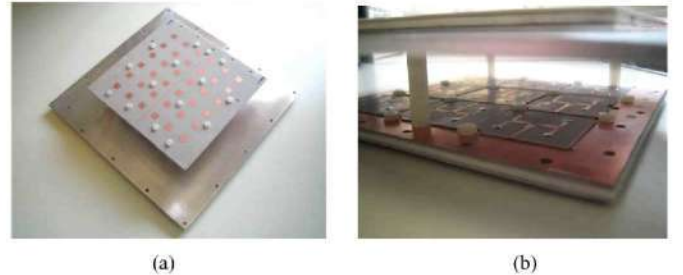
Fig. 22. Transmitarray core. (a) Radiating interfaces mounted together. (b) Distribution network integration.

Details of the assembly process are depicted in Figs. 22 and 23. Fig. 24 shows the transmitarray mounted in anechoic chamber for measurement acquisition.

All the phase shifters were measured and calibrated before the lens assembly. Results are shown in Table II. According to the values in Table II, a complete set of polarization voltages for each shifter is defined, depending on the phase shift desired at each four-patch group.

Analysis of Table II shows that, for the same voltage, there is a possible variation between shifters of around 30 deg. However, this error is not the one to be considered in the configuration, as each phase shifter is independently calibrated. For the sake

Voltage	Φ_1	Φ_2	Φ_3	Φ_4	Φ_5	Φ_6	Φ_7	Φ_8	Φ_9
0.0	0	0	0	0	0	0	0	0	0
-0.5	-4	-5	-5	-4	-4	-4	-5	-4	-4
-1.0	-10	-13	-11	-10	-12	-10	-10	-11	-10
-1.5	-20	-19	-20	-19	-20	-18	-18	-20	-20
-2.0	-31	-32	-29	-28	-32	-28	-26	-30	-34
-2.5	-44	-44	-42	-39	-43	-37	-37	-41	-44
-3.0	-60	-56	-55	-50	-58	-50	-51	-52	-60
-3.5	-77	-66	-67	-63	-71	-63	-65	-66	-77
-4.0	-94	-78	-82	-75	-84	-77	-78	-81	-94
-4.5	-111	-94	-98	-88	-102	-91	-93	-95	-108
-5.0	-130	-107	-114	-102	-115	-103	-104	-107	-127
-5.5	-145	-121	-130	-116	-130	-118	-120	-124	-145
-6.0	-161	-136	-144	-130	-144	-133	-133	-139	-161
-6.5	-175	-153	-159	-145	-157	-148	-148	-152	-175
-7.0	-187	-170	-173	-159	-174	-160	-160	-166	-187
-7.5	-202	-181	-187	-169	-186	-173	-173	-181	-201
-8.0	-218	-194	-200	-183	-200	-189	-189	-196	-215
-8.5	-228	-208	-217	-197	-214	-201	-199	-210	-227
-9.0	-235	-220	-227	-210	-229	-214	-210	-224	-235
-9.5	-247	-233	-242	-220	-241	-227	-225	-236	-247
-10.0	-263	-244	-256	-234	-256	-239	-234	-248	-263
-10.5	-275	-259	-269	-248	-270	-252	-249	-264	-274
-11.0	-288	-271	-283	-261	-284	-262	-260	-276	-288
-11.5	-300	-282	-297	-276	-298	-275	-270	-291	-299
-12.0	-310	-294	-310	-286	-309	-287	-280	-304	-308
-12.5	-323	-306	-322	-297	-320	-298	-291	-315	-321
-13.0	-334	-315	-336	-308	-329	-307	-301	-324	-334
-13.5	-345	-326	-343	-317	-338	-318	-309	-332	-346
-14.0	-353	-335	-354	-328	-348	-326	-318	-344	-353
-14.5	-364	-344	-363	-336	-356	-337	-324	-351	-364
-15.0	-373	-354	-372	-346	-365	-344	-336	-360	-372
-15.5	-381	-362	-382	-354	-371	-353	-341	-367	-381

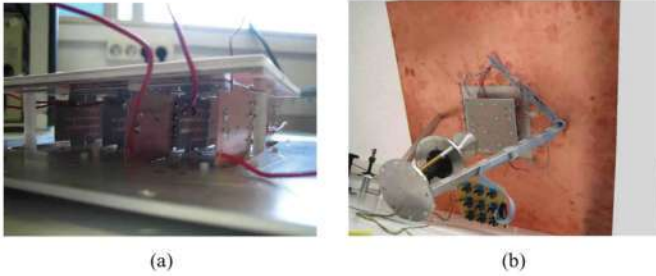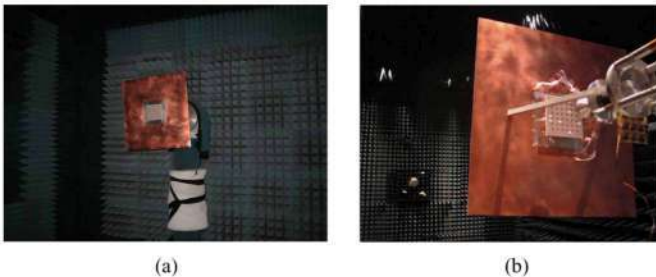Fig. 23. Assembly. (a) Phase shifter integration. (b) Complete transmitarray.

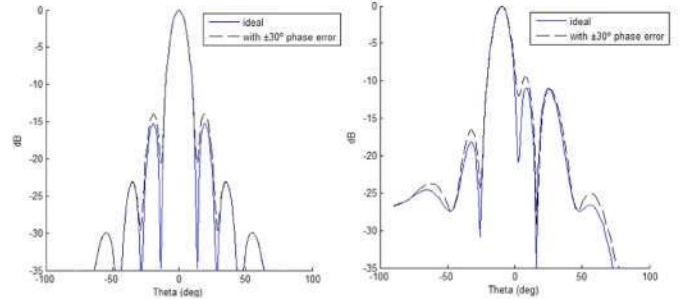Fig. 24. Transmitarray in anechoic chamber, different views.

Fig. 25. Comparison between the ideal case and a case with phase errors (worst case: Each shifter alternatively with $+30°$ or $-30°$ phase error), for simulated radiation patterns for steering angles of 0 deg and 9 deg.

radiation pattern degradation (steering direction and side lobe level) is still negligible, as it is observed in Fig. 25.

For prototype validation, two working configurations for the lens measurement are defined as follows.

- Pattern 1: The lens does not change the radiation pattern; it only corrects the phase error (all the phase shifters with the same polarization voltage, 0 V).
- Pattern 2: The lens changes the radiation pattern in one of the main axes, applying a 9-degree tilt. The required phase and voltage (after the calibration process) for each phase shifter are shown in Table III (shifters are ordered in columns, from top left to bottom right, in the square 3×3 grid of four-cell groups).

of completeness, a random ±30 deg phase error is introduced in the phase shifters and the radiation pattern is evaluated. The

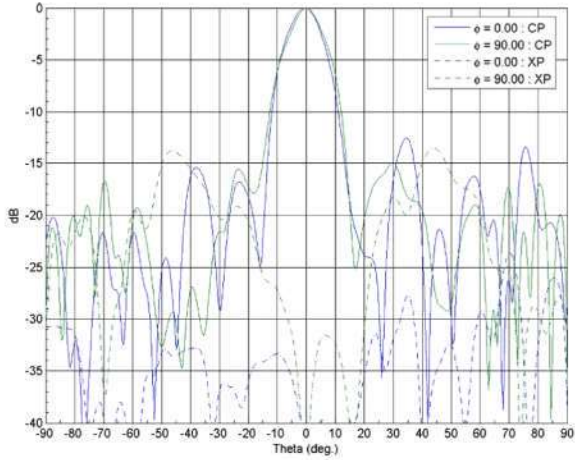|	Φ_1	Φ_2	Φ_3	Φ_4	Φ_5	Φ_6	Φ_7	Φ_8	Φ_9
Required Phase (deg)	-174	-174	-174	-87	-87	-87	0	0	0
Applied Voltage (V)	-6.5	-7.1	-7.0	-4.5	-4.1	-4.3	0	0	0

Fig. 26. Transmitarray measurement results for the steering angle of 0 deg.
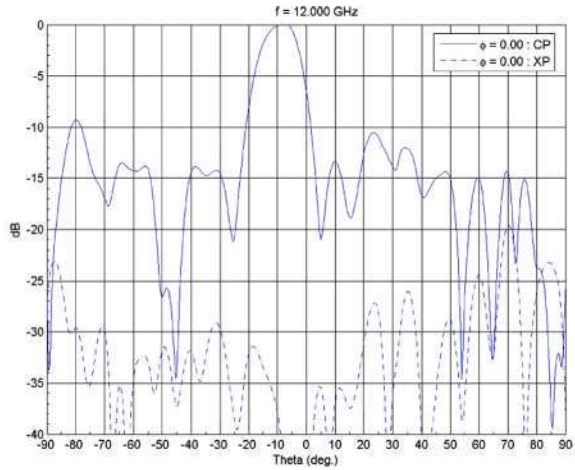

Fig. 27. Transmitarray measurement results for the steering angle of 9 deg.

Results for both configurations are offered in Figs. 26 and 27. These patterns are well compared with the theoretical results shown in Fig. 25.

With these results, it is convenient to analyze measured gain results and expected directivity values. Measurements yield 21.6 dBi in directivity. The measured results provide 16 dBi mean value in gain. The reduction is due to the accepted horn power (60% (-2.2 dB) in this case, due to spillover) and processing interface insertion losses (3 dB mean value, due to phase shifters), as expected.

VII. CONCLUSION

In this work, a complete electronically reconfigurable transmitarray device has been presented. Some theoretical background and architecture considerations were offered and

adequate architecture was chosen and adapted in order to allow the integration of active circuitry in the complete lens design.

A complete active transmitarray was designed, manufactured, assembled and measured in an anechoic chamber. Due to some constraints (space and cost of the first prototype), patches were grouped into sets of four and each group phase behavior was controlled by one $> 360°$ phase shifter that was electronically reconfigurable. This yielded a more limited reconfigurable global device (possible problems with grating lobes and its radiation), but was valid for a first active transmitarray prototype. Design and manufacture considerations have been mentioned and a 36-element array device was manufactured. For this purpose, nine phase shifters were built, measured and characterized before being integrated into the lens. Once the first prototype was assembled, two configurations were defined in order to achieve the proper behavior of the transmitarray prototype. Prototype measurements in anechoic chamber were obtained and main features (gain, directivity, etc.) were extracted.

REFERENCES

[1] D. McGrath, "Planar three-dimensional constrained lenses," *IEEE Trans. Antennas Propag.*, vol. 34, pp. 46–50, Jan. 1986.
[2] P. J. Kahrilas and D. M. Jahn, "Hardpoint demonstration array radar," *IEEE Trans. Aerosp. Electron. Syst.*, vol. AES-2, pp. 286–299, Nov. 1966.
[3] P. J. Kahrilas, "HAPDAR—An operational phased array radar," *Proc. IEEE*, vol. 56, pp. 1967–1975, Nov. 1968.
[4] J. Vian and Z. Popovic, "Smart lens antenna arrays," presented at the IEEE Microwave Symp., 2001.
[5] A. Muñoz-Acevedo, P. Padilla, and M. Sierra-Castañer, "Ku band active transmitarray based on microwave phase shifters," presented at the Eur. Conf. on Antennas and Propagation (EuCAP 2009), Berlin, Germany, Mar. 2009.
[6] M. Barba, E. Carrasco, and J. A. Encinar, "Suitable planar transmit-arrays in X-band," presented at the Eur. Conf. on Antennas and Propagation (EuCAP 2006), Nov. 2006.
[7] P. Padilla and M. Sierra-Castañer, "Design and prototype of a 12 GHz transmit-array," *Microw. Opt. Technol. Lett.*, vol. 49, no. 12, pp. 3020–3026, Dec. 2007.
[8] J. Costa, C. Fernandes, G. Godi, R. Sauleau, L. Le Coq, and H. Legay, "Compact ka-band lens antennas for LEO satellites," *IEEE Trans. Antennas Propag.*, vol. 56, pp. 1251–1258, May 2008.
[9] S. Hopfer, "Analog phase shifter for 8–18 GHz," *Microw. J.*, vol. 22, pp. 48–50, Mar. 1979.
[10] W. Hoefer, "Equivalent series inductivity of a narrow transverse slit in microstrip," *IEEE Trans. Microw. Theory Tech.*, vol. 25, pp. 822–824, Oct. 1977.
[11] R. Chadha and K. Gupta, "Compensation of discontinuities in planar transmission lines," *IEEE Trans. Microw. Theory Tech.*, vol. 82, pp. 2151–2156, Dec. 1982.

[12] C. Balanis, *Advanced Engineering Electromagnetics*. New York: Wiley, 1989.

[13] D. Pozar, *Microwave Engineering*, 3rd ed. Hoboken, NJ: Wiley, 2004.

[14] E. O. Hammerstad, "Equations for microstrip circuit design," in *Proc. 5th Eur. Microwave Conf.*, Oct. 1975, pp. 268–272.

[15] P. Padilla and M. Sierra-Castañer, "Transmitarray for Ku band," presented at the Eur. Conf. on Antennas and Propagation (EuCAP 2007), Edinburgh, U.K., Nov. 2007.

[16] P. Padilla and M. Sierra-Castañer, "Design of a 12 GHz transmit-array," presented at the IEEE AP-S Int. Symp. on Antennas and Propagation (APS 2007), Hawaii, Jun. 2007.

[17] E. Fotheringham, S. Rómisch, P. C. Smith, D. Popovic, D. Z. Anderson, and Z. Popovic, "A lens antenna array with adaptative optical processing," *IEEE Trans. Antennas Propag.*, vol. 50, May 2002.

[18] D. Popovic and Z. Popovic, "Multibeam antennas with polarization and angle diversity," *IEEE Trans. Antennas Propag.*, vol. 50, pp. 651–657, May 2002.

[19] Z. Popovic and A. Mortazawi, "Quasi-Optical transmit/receive front end," *IEEE Trans. Microw. Theory Tech.*, vol. 46, Nov. 1998.

[20] S. Hopfer, "Analog phase shifter," U.S. patent 4288763.

[21] A. Malczewski, S. Eshelman, B. Pillans, J. Ehmke, and C. Goldsmith, "X-band RF MEMs phase shifters for phased array applications," *IEEE Microw. Guided Wave Lett.*, vol. 9, pp. 517–519, Dec. 1999.

[22] B. Pillans, S. Eshelman, A. Malczewski, J. Ehmke, and C. Goldsmith, "Ka-band RF MEMs phase shifters," *IEEE Microw. Guided Wave Lett.*, vol. 9, pp. 520–522, Dec. 1999.

Alfonso Muñoz-Acevedo was born in Toledo, Spain, in 1985. He received the Telecommunication Engineer degree from the Technical University of Madrid (UPM), Spain, in 2008, where he is currently working toward the Ph.D. degree.

Since September 2007, he has been with the Radiation Group of the Signal, Systems and Radiocommunications Department of UPM. His research interests include antenna design and synthesis and the area of active microwave and millimeter wave devices.

Manuel Sierra-Castañer (M'95) was born in Zaragoza, Spain, in 1970. He received the Telecommunication Engineer degree in 1994 and the Ph.D. degree in 2000, both from Technical University of Madrid, in Madrid, Spain.

Since 1997, he has been at the University "Alfonso X" as a Teaching Assistant, and since 1998, at the Technical University of Madrid as a Research Assistant, Assistant and Associate Professor. His current research interests are in planar antennas and antenna measurement systems.

Pablo Padilla was born in Jaén, south of Spain, in 1982. He received the Telecommunication Engineer degree and the Ph.D. degree both from Technical University of Madrid (UPM), Spain, in 2005 and 2009, respectively.

From September 2005 to September 2009, he was with the Radiation Group of the Signal, Systems and Radiocommunications Department, UPM. In 2007, he was with the Laboratory of Electromagnetics and Acoustics at Ecole Polytechnique Fédérale de Lausanne (EPFL), Switzerland, as an invited Ph.D. Student. Currently, he is Assistant Professor at Universidad de Granada (UGR) and collaborates with the Radiation Group of the Technical University of Madrid. His research interests include antenna design and synthesis and the area of active microwave devices.

Manuel Sierra-Pérez (M'78–SM'07) was born in Zaragoza, Spain, in 1952. He received the Master's and Ph.D. degrees from Technical University of Madrid, in Madrid, Spain, in 1975 and 1980, respectively.

He became a Full Professor with the Department of Signals, Systems and Radio Communications at the Technical University of Madrid in 1990. He was an Invited Professor at the National Radio-Astronomy Observatory (NRAO), VA, from 1981 to 1982, and at the University of Colorado at Boulder, from 1994 to 1995. His current research interest is in passive and active array antennas, including design theory, measurement, and applications.

Dr. Sierra-Pérez was a promoter and Chairman of the IEEE joint AP/MTT Spanish Chapter. He was Treasurer of the IEEE Spain Section and has been President of the same section since 2008.